X-ray and neutron scattering from rough surfaces

S. K. Sinha, E. B. Sirota, and S. Garoff*

*Corporate Research Science Laboratory, Exxon Research and Engineering Company, Clinton Township, Route 22 East,
Annandale, New Jersey 08801*

H. B. Stanley[†]
University of Maryland, College Park, Maryland 20742

The scattering of x rays and neutrons from rough surfaces is calculated. It is split into specular reflection and diffuse scattering terms. These are calculated in the first Born approximation, and explicit expressions are given for surfaces whose roughness can be described as self-affine over finite length scales. Expressions are also given for scattering from liquid surfaces, where it is shown that "specular" reflections only exist by virtue of a finite length cutoff to the mean-square height fluctuations. Expressions are also given for the scattering from randomly oriented surfaces, as studied in a typical small-angle scattering experiment. It is shown how various well-known asymptotic power laws in $S(q)$ are obtained from the above theory. The distorted-wave Born approximation is next used to treat the case where the scattering is large (e.g., near the critical angle for total external reflection), and its limits of validity are discussed. Finally, the theory is compared with experimental results on x-ray scattering from a polished Pyrex glass surface.

I. INTRODUCTION

The scattering of radiation by surfaces or interfaces possessing roughness has been the object of study of a large body of work.[1-15] Most of this work has been concerned with the scattering of light or radar waves by rough surfaces, where the interaction between the radiation and the scattering material is very strong. As is well known, this is a very difficult problem, amounting to finding approximations for solving the standard equations of electromagnetic theory, while matching boundary conditions over a random surface. It is known that the reflection of x rays from surfaces yields information about surface roughness and the same is true for the analogous case of neutrons. In this case, we are quite often in the weakly interacting approximation. Thus, one may think of the Born approximation as the starting point to discuss the scattering. The wavelength of such radiation (1–8 Å) enables one to study microscopic details of the roughness on comparable length scales. Many experiments to date have reported on the specularly reflected component of the scattering and this component has usually been analyzed as the Fresnel reflectivity multiplied by a "Debye-Waller factor" from which the mean-square surface roughness can be deduced.[1,3,16-21] There has been less experimental or theoretical work to date on the diffuse (nonspecular) component of the scattering which is related to the height-height correlation function of the rough surface. It turns out that an estimate of the diffuse scattering is important even in estimating the specular reflectivity when the latter becomes small, since the diffuse scattering becomes comparable to or greater than the specular, at large angles and finite resolution.

On the other hand, there has been a large body of parallel work discussing the small-angle scattering from systems which are homogeneous except for possessing internal or external surfaces.[22] This has been done within the Born approximation and, for the case where the surfaces are smooth (on the scale of the inverse of the wavevector transfer q), yields the well-known Debye-Porod q^{-4} law for the asymptotic form of the scattering. Recently, the Debye-Porod law has been extended (for scattering from systems with randomly oriented surfaces) to the case of scattering from fractal[23] or self-affine[24] surfaces, each yielding a characteristic asymptotic power law in q.

The plan of the paper is as follows: In Sec. II, we shall use the Born approximation to discuss scattering from a single rough surface. We shall show how the scattering splits up naturally into a specular and diffuse part. The explicit expressions for the diffuse scattering from single solid and liquid surfaces are derived for use in analyzing experimental data. In Sec. III, we show how randomly averaging over all directions yields well known and previously derived asymptotic power laws for specific kinds of roughness. The Born approximation breaks down as we approach the regime of total reflection, however, and thus, in Sec. IV, we discuss the use of the distorted-wave Born approximation (DWBA) to treat the problem. In this method, one exploits the fact that the actual rough surface represents a small perturbation from the smooth surface, for which the exact solution is known from standard Fresnel theory. One may therefore use the exact eigenfunctions for the case of the smooth surface as basis functions for carrying out the perturbation theory. The DWBA yields an expression for the specular reflectivity which is very similar to a previously derived expression for the latter,[21] provided $q_z \sigma$ does not become $\gg 1$, where σ is the root-mean-square (rms) surface roughness and q_z is the specular component of the wave-vector

transfer. It also yields a simple modification for the diffuse scattering given by the Born approximation, whose most striking effect is to yield a peak in the scattering, whenever the incident or scattered rays make the critical angle of incidence with the surface normal.[25] The DWBA, however, also has its limitations for calculations of the specular reflectivity and in Sec. IV we also discuss critically the limits of validity of this approximation.

In Sec. V we present experimental results for the x-ray specular and diffuse reflectivity from a polished glass surface and an analysis in terms of the model outlined above. Because synchrotron radiation was employed, we are able to measure to at least eight orders or magnitude down from the specular total reflection, which enables one to make a stringent test of models for both specular and diffuse scattering.

II. SCATTERING IN THE BORN APPROXIMATION

Let us assume that the material is homogeneous on the length scale being probed, except for the presence of a surface. This means that atomic structure will be ignored. This is a valid approximation as long as we are dealing with small angle scattering where the condition $qa \ll 1$ is satisfied, where q ($=4\pi \sin\theta/\lambda$, 2θ being the scattering angle and λ being the wavelength of the radiation) is the wave-vector transfer and a is a typical length scale for any inhomogeneity within the solid.

The differential cross section for scattering of the radi-

ation by a system is then given in the Born approximation by

$$\frac{d\sigma}{d\Omega} = N^2 b^2 \int_V d\mathbf{r} \int_V d\mathbf{r}' \, e^{-i\mathbf{q}\cdot(\mathbf{r}-\mathbf{r}')} , \qquad (2.1)$$

where b is a characteristic scattering length and N is the number density of the scattering particles. For neutron scattering, b is the coherent scattering length of the nuclei and for x-ray scattering $b = (e^2/mc^2)$, the Thompson scattering length of the electron. The integrals are over the volume of the solid and

$$\mathbf{q} \equiv \mathbf{k}_2 - \mathbf{k}_1 , \qquad (2.2)$$

where $\mathbf{k}_1$ and $\mathbf{k}_2$ are the incident and scattered wave vectors, respectively. The volume integrals in Eq. (2.1) may be transformed into surface integrals to yield

$$\frac{d\sigma}{d\Omega} = N^2 b^2 \frac{1}{(\mathbf{q}\cdot\mathbf{A})^2} \int_S \int_S (d\mathbf{S}\cdot\mathbf{A})(d\mathbf{S}'\cdot\mathbf{A}) e^{-i\mathbf{q}\cdot(\mathbf{r}-\mathbf{r}')} , \qquad (2.3)$$

where $\mathbf{A}$ is an arbitrary unit vector in space and $d\mathbf{S}$ represents the differential surface vector parallel to the surface normal. Let us consider a rough surface as indicated schematically in Fig. 1, which has associated with it an *average* smooth surface. The latter will be chosen as the (x,y) plane. Let us choose $\mathbf{A}$ to be the unit vector $\hat{z}$. Then Eq. (2.3) may be written as

$$\frac{d\sigma}{d\Omega} = \frac{N^2 b^2}{q_z^2} \int \int_{S_0} dx\, dy \int \int_{S_0} dx'\, dy' \exp\{-iq_z[z(x,y)-z(x',y')]\} \exp\{-i[q_x(x-x')+q_y(y-y')]\} , \qquad (2.4)$$
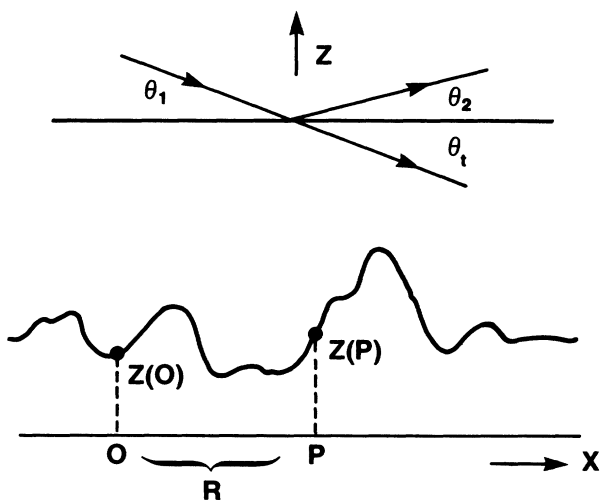

FIG. 1. Schematic of a rough surface. z is the normal to the surface. x is along the average surface in the specular scattering plane. θ_1 is the *grazing* angle of incidence, θ_2 is the *grazing* angle of reflection, and θ_t is the *grazing* angle of refraction. $z(P)$ is the height of the surface at point P. At specular $\theta_1 = \theta_2$.

where S_0 is the surface of the (x,y) plane and $z(x,y)$ (assumed to be single valued) is the height of the surface above the plane at the coordinates (x,y). We now make the central assumption that $[z(x',y')-z(x,y)]$ is a Gaussian random variable whose distribution depends on the relative coordinates $(X,Y) \equiv (x'-x, y'-y)$. Specifically we write

$$\langle [z(x',y')-z(x,y)]^2 \rangle = g(X,Y) , \qquad (2.5)$$

where the average is taken over all pairs of points on the surface whose (x,y) coordinates are separated by (X,Y) (see Fig. 1).

For many isotropic solid surfaces we may represent $g(X,Y)$ by

$$g(X,Y) = g(R) = AR^{2h} \quad (0 < h < 1) , \qquad (2.6)$$

where $R \equiv (X^2+Y^2)^{1/2}$. This kind of roughness is associated with the self-affine surface defined by Mandelbrot[26] in terms of fractional Brownian motion. Computer simulations of such surfaces by Voss[27] show remarkable similarity to various kinds of physical surfaces, both microscopic and macroscopic. The exponent determines how

smooth or jagged (subjectively speaking) such a surface is. Thus, small values of h produce extremely jagged surfaces, while values of h approaching 1 appear to have "smooth" hills and valleys. h thus determines the texture of the roughness. For self-affine rough surfaces, the property of self-similarity peculiar to true fractals does not appertain, since the z direction scales differently to the x,y directions. At large enough distances the surface looks flat, since $|z(R)-z(0)|/R \to 0$ as $R \to \infty$, but at length scales $\ll R_0$, where

$$R_0 \equiv A^{1/2(1-h)} \qquad (2.7)$$

the surface looks like a fractal surface, with surface fractal dimension given by[26,27]

$$D_s = 3 - h \ . \qquad (2.8)$$

The reader is referred to a discussion of this point by Alexander.[28] Equation (2.6) represents an idealization, as the function $g(R)$ diverges at infinity. In practice the mean-square roughness may saturate at a value σ^2 for many reasons, finite size being one such reason. Accordingly we write

$$g(R) = 2\sigma^2[1 - e^{-(R/\xi)^{2h}}] \qquad (2.9)$$

which for $R \ll \xi$ has the same form as Eq. (2.6). ξ is an effective cutoff length for the roughness of the form given in Eq. (2.6). The crossover length defined in Eq. (2.7) is now given by

$$R_0 = (\sqrt{2}\sigma/\xi^h)^{1/(1-h)} \ . \qquad (2.10)$$

Assuming here, that $[z(x,y)-z(x',y')]$ is a Gaussian random variable, we may write, for an area $(L_x L_y)$ of the reference surface, from Eq. (2.4)

$$\frac{d\sigma}{d\Omega} = \frac{N^2 b^2}{q_z^2} L_x L_y \int \int_{S_0} dX\, dY\, e^{-q_z^2 g(X,Y)/2} e^{-i(q_x X + q_y Y)} \ . \qquad (2.11)$$

We may now obtain explicit expressions for $S(\mathbf{q})$, defined as the (cross section per unit area surface)/$(N^2 b^2)$, for various models of $g(R)$.

A. Smooth surfaces

If the surface is completely smooth, $g(R)=0$, and Eq. (2.11) yields

$$S(\mathbf{q}) \equiv \frac{d\sigma}{d\Omega} \frac{1}{N^2 b^2 L_x L_y} = \frac{4\pi^2}{q_z^2} \delta(q_x)\delta(q_y) \ . \qquad (2.12)$$

The delta functions contain the conditions for specular reflection. The absolute value of the square of the reflectivity, [defined as (reflected intensity)/(incident intensity)], is obtained as

$$|R|^2 = \frac{1}{L_x L_y \sin\theta_1} \int \left[\frac{d\sigma}{d\Omega}\right]_{spec} d\Omega \ , \qquad (2.13)$$

where $d\Omega$ is a unit element of solid angle for the scattered beam, and the factor $1/\sin\theta_1$ allows for the fact that cross sections are defined in terms of incident flux,

but reflectivities are defined in terms of total intensity. The angles θ_1 and θ_2 represent the angles made with the average smooth surface by the incident and scattered beams, respectively (see Fig. 1). Now for elastic scattering,

$$d\Omega = \frac{dq_x\, dq_y}{k_0^2 \sin\theta_2} \ , \qquad (2.14)$$

where k_0 is the magnitude of the wave vector of the incident radiation. Thus, from Eqs. (2.12)–(2.14), we get the specular reflectivity for a smooth surface

$$|R|^2 = \frac{16\pi^2 N^2 b^2}{q_z^4} \ . \qquad (2.15)$$

Using the definition of the refractive index of the medium

$$n = 1 - bN\lambda^2/2\pi \ , \qquad (2.16)$$

Eq. (2.15) can be cast in the form

$$|R|^2 = \left[\frac{(1-n^2)}{4\sin^2\theta_1}\right]^2 \qquad (2.17)$$

which is consistent with the large θ asymptotic limit of the usual Fresnel theory. In deriving Eq. (2.17) we have used the fact that $(n-1)$ is a very small quantity (typically $\sim 10^{-6}$). Equation (2.12) is essentially equivalent to Porod's law as we shall see in Sec. II. It has not generally been realized that the Fresnel theory and Porod's law (both valid for smooth surfaces) are equivalent formulations of the same results for large incident angles.

B. Rough surfaces with no cutoff

Let us now consider an isotropic rough surface. Equation (2.11) may be expressed more conveniently in terms of q_z and q_r,

$$S(\mathbf{q}) = \frac{2\pi}{q_z^2} \int_0^\infty dR\, Re^{-q_z^2 g(R)/2} J_0(q_r R) \ , \qquad (2.18)$$

where $q_r \equiv (q_x^2 + q_y^2)^{1/2}$. For the case of $g(R)$ given by Eq. (2.6) (i.e., with no cutoff for the mean-square height deviations), there is no delta function in q_x or q_y, i.e., no true specular component. All of the intensity can be regarded as diffuse scattering. Equation (2.18) may be written as

$$S(\mathbf{q}) = \frac{2\pi}{q_z^2} \int_0^\infty dR\, Re^{-(A/2)q_z^2 R^{2h}} J_0(q_r R) \ . \qquad (2.19)$$

This cannot, in general, be calculated analytically, except for special cases:

for $h = \frac{1}{2}$, $\quad S(\mathbf{q}) = \dfrac{A\pi}{(q_r^2 + (A/2)^2 q_z^4)^{3/2}} \qquad (2.20)$

and

for $h = 1$, $\quad S(\mathbf{q}) = \dfrac{2\pi}{A q_z^4} e^{-q_r^2/2 A q_z^2} \ . \qquad (2.21)$

However, at specular (i.e., when $q_r = 0$), Eq. (2.19) can always be evaluated to yield

$$[S(\mathbf{q})]_{[q_r=0]} = \frac{2\pi Q_h(A)}{q_z^{2+2/h}} , \qquad (2.22)$$

where

$$Q_h(A) = \int_0^\infty d\xi\, \xi e^{-(A/2)\xi^{2h}} .$$

Equation (2.22) shows that the asymptotic form of the *diffuse* scattering at the specular condition has a power-law form in q, whose exponent is related to the surface roughness exponent h. This will be true even if there is a long length-scale cutoff for $g(R)$.

C. Rough surfaces with cutoff

Let us investigate the effect of using the cutoff form [Eq. (2.9)] for $g(R)$. Note that by Eq. (2.5),

$$g(X,Y) = 2\langle z^2\rangle - 2\langle z(X,Y)z(0,0)\rangle . \qquad (2.23)$$

If we write $\langle z^2\rangle = \sigma^2$, we have, for the height-height correlation function $C(X,Y)$,

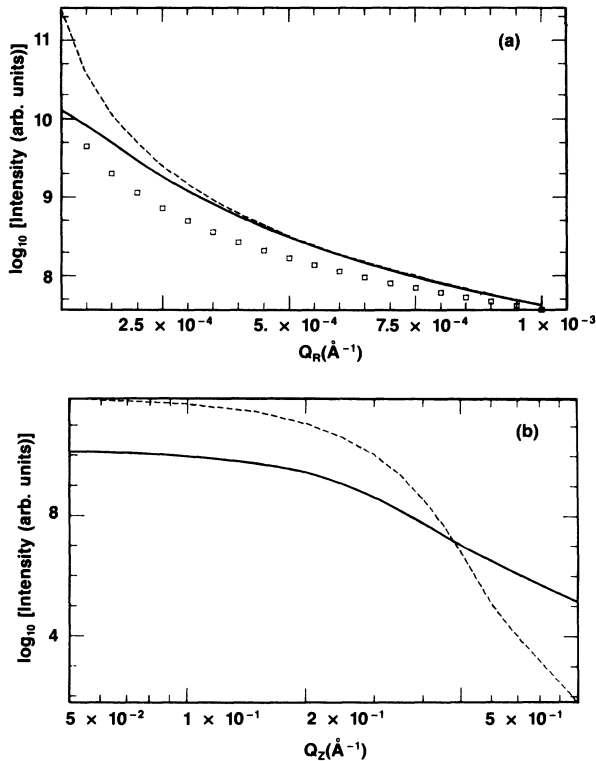$$C(X,Y) \equiv \langle z(X,Y)z(0,0)\rangle = \sigma^2 - \tfrac{1}{2}g(X,Y) \qquad (2.24)$$

FIG. 2. Calculated $S_{\text{diff}}(\mathbf{q})$ as calculated from the equations given in the text. (a) $S(q)$ vs q_r (in Å^{-1}) for $q_z=0.01\ \text{Å}^{-1}$. Solid line represents the case where $h=0.5$, $\sigma=7\ \text{Å}$, $\xi=7000\ \text{Å}$; dashed line represents the case with no cutoff; open squares represent the case where $h=0.2$, $\sigma=7\ \text{Å}$, $\xi=7000\ \text{Å}$. (b) $S(q)$ vs q_z (in Å^{-1}). Solid line represents case where $h=0.5$, $\sigma=7\ \text{Å}$, $\xi=7000\ \text{Å}$; dashed line represents case where $h=0.2$, $\sigma=7\ \text{Å}$, $\xi=7000\ \text{Å}$. For longitudinal (q_z) scans, the shape of $S(q)$ is unaffected by ξ.
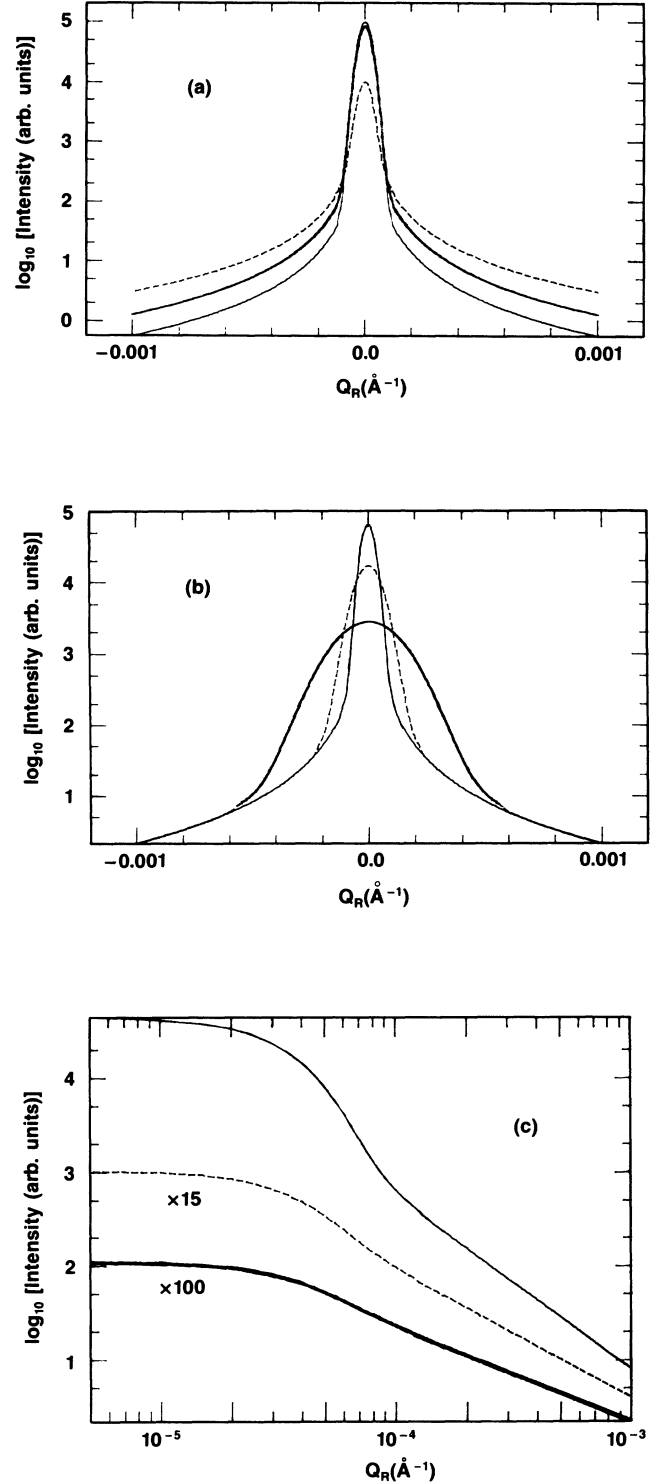

FIG. 3. Calculated intensity vs q_r using Eq. (2.33) with $A=0$. (a) $q_z=0.3\ \text{Å}^{-1}$, $\zeta=1\times10^5\ \text{Å}$, $B=0.2$ (solid line), $B=0.5$ (bold line), $B=5.0$ (dashed line). Note the variation in peak-to-tail ratio. (b) $q_z=0.3\ \text{Å}^{-1}$, $B=1.0$, $\zeta=1\times10^5\ \text{Å}$ (solid line), $\zeta=5\times10^4\ \text{Å}$ (dashed line), $\zeta=2\times10^4\ \text{Å}$ (bold line). Note the variation in the central peak width. (c) log-log plot showing the different values for the limiting slope where $B=8$, $\zeta=1\times10^5\ \text{Å}$, $q_z=0.2\ \text{Å}^{-1}$ $\eta=0.16$ (solid line), $q_z=0.4\ \text{Å}^{-1}$ $\eta=0.64$ (dashed line) (scaled $\times15$), $q_z=0.5\ \text{Å}^{-1}$ $\eta=1.0$ (bold line) (scaled $\times100$).

and using the form chosen in Eq. (2.9) we obtain

$$C(X,Y)=\sigma^2 e^{-(R/\xi)^{2h}} . \tag{2.25}$$

Thus, from Eqs. (2.11) and (2.23)

$$S(\mathbf{q})=\frac{1}{q_z^2}e^{-q_z^2\sigma^2}\int\int_{S_0}dX\,dY\,e^{q_z^2 C(X,Y)}e^{-i(q_x X+q_y Y)} . \tag{2.26}$$

Let us write

$$F(q_z,R)\equiv e^{q_z^2 C(X,Y)}-1 . \tag{2.27}$$

By Eq. (2.25), $F\rightarrow 0$ as $R\rightarrow\infty$. Then, Eq. (2.26) splits into a specular and diffuse part. $S(\mathbf{q})=S_{\text{spec}}(\mathbf{q})+S_{\text{diff}}(\mathbf{q})$, where

$$S_{\text{spec}}(\mathbf{q})=\frac{4\pi^2}{q_z^2}e^{-q_z^2\sigma^2}\delta(q_x)\delta(q_y) \tag{2.28a}$$

and

$$S_{\text{diff}}(q)=\frac{2\pi}{q_z^2}e^{-q_z^2\sigma^2}\int_0^\infty dR\,RF(q_z,R)J_0(q_r R) , \tag{2.28b}$$

where

$$F(q_z,R)=\exp(q_z^2\sigma^2 e^{-(R/\xi)^{2h}})-1 . \tag{2.29}$$

The diffuse component must be evaluated numerically in general. However, the specular part is seen to simply multiply the expression for $|R|^2$ given in Eq. (2.15) by $\exp(-q_z^2\sigma^2)$. Figure 2 shows $S_{\text{diff}}(\mathbf{q})$ for various kinds of scans in (q_z,q_r) space, for different values of h, for the case where no cutoff is used and for a case where a cutoff value of 7000 Å is used. It is seen that for large q, the asymptotic behavior is independent of cutoff. For small q_z values, the Born approximation is invalid. In many experiments, the scattering is done with the instrumental resolution very wide in the transverse out-of-plane direction (in the plane of the surface, out of the scattering plane). (Let us call this the y direction.) Then, what is observed corresponds to

$$I(q_x,q_y)\propto\int S(\mathbf{q})dq_y=\frac{1}{q_z^2}\int dX\,e^{-q_z^2 g(X,0)/2}e^{-iq_x X} . \tag{2.30}$$

D. Liquid surfaces

In the case of liquid surfaces,[3,17,29] or purely two-dimensional systems, it is well known that, ignoring finite size effects, the capillary wave fluctuations[30] cause $g(R)$ to be given by a logarithmic form

$$g(R)=A+B\ln(R) \quad (R \text{ in } \text{Å}) . \tag{2.31}$$

Substituting in Eq. (2.18), we have

$$S(q)=\frac{2\pi}{q_z^2}e^{-q_z^2 A/2}\int_0^\infty dR\,RR^{-Bq_z^2/2}J_0(q_r R)$$

$$=\frac{2\pi}{q_z^2}e^{-q_z^2 A/2}\frac{2^{1-\eta}}{q_r^{2-\eta}}\frac{\Gamma(1-\eta/2)}{\Gamma(\eta/2)} , \tag{2.32}$$

where $\eta=Bq_z^2/2$. Again, there is no true specular component due to the divergence of $g(R)$ as $R\rightarrow\infty$. For actual experiments on liquids, finite size effects occur in two ways. One is that $g(R)$ does not diverge but cuts off at a finite value due to the cutoff of very long wavelength surface modes (by gravity or finite depth[30]). The other is that the integral in Eq. (2.32) does not extend over all R, but is cut off by the coherence of the scattering. The discussion is completely analogous to that given by Dutta and Sinha[31] where it is shown that the dominant effect is often the second one previously mentioned. The actual finite size in an x-ray scattering experiment will often be the coherence length ζ of the photon beam on the sample for the scattering geometry in question (typically microns, projected along the surface, of the sample under high resolution conditions). Thus, following Dutta and Sinha,[31] we write

$$S(q)\simeq\frac{2\pi}{q_z^2}e^{-q_z^2 A/2}\int_0^\infty dR\,R^{1-\eta}J_0(q_r R)e^{-\pi R^2/\zeta^2}$$

$$=\frac{1}{q_z^2}e^{-q_z^2 A/2}\Gamma(1-\eta/2)\pi^{\eta/2}\zeta^{2-\eta}\Phi[(1-\eta/2);1;-q_r^2\zeta^2/4\pi] , \tag{2.33}$$

where η is defined in Eq. (2.32) and Φ is the Kummer function.[32] Note that η itself is a function of q_z.

For $q_r\leq 1/\zeta$, $S(\mathbf{q})$ has the form

$$S(\mathbf{q})\simeq\frac{1}{q_z^2}e^{-q_z^2 A/2}e^{-(1-\eta/2)q_r^2\zeta^2/4\pi}\Gamma(1-\eta/2)\pi^{\eta/2}\zeta^{2-\eta} . \tag{2.34}$$

For $q_r\gg 1/\zeta$, $S(\mathbf{q})$ reduces to the form given in Eq. (2.32). Figure 3 shows calculations of $S(\mathbf{q})$ from the surface of a liquid for various values of the parameters B, q_z, and ζ.

For the case where the scattering is limited by the gravitational cutoff of the capillary waves, $g(R)$ is given by the form

$$g(R)=\sigma^2(1-K_0(\kappa R)) , \tag{2.35}$$

where κ is an inverse cutoff length and K_0 is a Bessel function which goes to zero for large values of the argument and

behaves logarithmically [as in Eq. (2.31)] for small values of the argument. In this case there *is* a truly specular component given by Eq. (2.28a) and a diffuse component given by

$$S_{\text{diff}}(q) = \frac{2\pi}{q_z^2} e^{-q_z^2\sigma^2/2} \int_0^\infty R\,dR\, J_0(q_r R)(e^{(q_z^2\sigma^2/2)K_0(\kappa R)} - 1) \ . \tag{2.36}$$

In the limit that $q_z\sigma \to 0$ this reduces to

$$S_{\text{diff}}(q) = \frac{\pi\sigma^2}{q_r^2 + \kappa^2} \tag{2.37}$$

and for $q_r \gg \kappa$, for all q_z

$$S_{\text{diff}}(q) \approx \frac{2\pi}{q_z^2}\kappa^{-\eta}e^{-\eta}\frac{2^{1-\eta}}{q_r^{2-\eta}}\frac{\Gamma(1-\eta/2)}{\Gamma(\eta/2)} \quad \text{with } \eta = q_z^2\sigma^2/2 \tag{2.38}$$

which is equivalent to Eq. (2.32) since the cutoff is irrelevant at large q_r.

III. SMALL-ANGLE SCATTERING FROM RANDOMLY ORIENTED ROUGH SURFACES

Small-angle scattering from surfaces is often carried out in the case where the surfaces in the sample being studied are randomly oriented with respect to the wave vector q, as in a powder. The Born approximation is usually assumed to be valid. In what follows, we assume, as we did in Sec. II, that q is large enough so that (a) the scattering is weak and the Born approximation is valid and that (b) the surfaces are locally *flat* (but not necessari-

ly smooth) on a length scale $\leq 1/q$, i.e., an *average* smooth surface can be defined on such length scales. We may then obtain $\tilde{S}(q)$, by averaging the results in the preceding section over all directions of q,

$$\tilde{S}(q) = \frac{1}{4\pi}\int\int S(\mathbf{q})\sin\chi\,d\chi\,d\phi\ , \tag{3.1}$$

where χ and ϕ are the polar angles of the vector q relative to the local axes as defined in Fig. 1.

For a fixed magnitude of q,

$$\sin\chi\,d\chi\,d\phi = \frac{dq_x\,dq_y}{q^2\cos\chi}\ . \tag{3.2}$$

Thus, for a smooth surface, Eq. (2.12) yields

$$\tilde{S}(q) = \frac{2\pi}{q^4} \tag{3.3}$$

which is Porod's law.[22] [We note that from the expression Eq. (2.3) for $d\sigma/d\Omega$, that the scattering is the same whether the incident beam impinges on the surface from inside or outside the medium. Thus, the range of integration in Eq. (3.1) for χ is $0 \to \pi$ instead of $0 \to \pi/2$.] For a surface roughness characterized by a $g(R)$ function [Eq. (2.5)] given by either Eq. (2.6) or (2.9), we have by Eq. (2.18),

$$\tilde{S}(q) = \frac{\pi}{q^2}\int_0^\pi d\chi\,\frac{\sin\chi}{\cos^2\chi}\int_0^\infty dR\ Re^{-q^2\cos^2\chi g(R)/2}J_0(qR\sin\chi)$$

$$= \frac{\pi}{q^2}\int_{-1}^{+1}\frac{dy}{y^2}\int_0^\infty dR\ Re^{-q^2y^2g(R)/2}J_0[qR(1-y^2)^{1/2}]\ . \tag{3.4}$$

We may change variable in the argument of the Bessel function and explicitly use Eq. (2.6) to obtain in the case where we neglect a cutoff for the roughness,

$$\tilde{S}(q) = \frac{\pi}{q^4}\int_{-1}^1\frac{dy}{y^2}\int_0^\infty R'\,dR'\,e^{-y^2q^{2-2h}(R')^{2h}/2}J_0[R'(1-y^2)^{1/2}]\ . \tag{3.5}$$

We now substitute for the variable y, the variable $y' = q^{1-h}y$ to obtain

$$\tilde{S}(q) = \frac{\pi}{q^{3+h}}\int_{-q^{1-h}}^{+q^{1-h}}\frac{dy'}{y'^2}\int_0^\infty dR'\,R'e^{-(y')^2(R')^{2h}/2}J_0\{R'[1-(y')^2/q^{2-2h}]^{1/2}\}\ . \tag{3.6}$$

Now we recognize that in this integral, the main contribution will arise from small values of y'. Accordingly, as q becomes asymptotically large, the integral will tend to

$$\tilde{S}(q) \simeq \frac{\pi}{q^{3+h}}\int_{-\infty}^{+\infty}dy'\int_0^\infty dR'\,\frac{R'}{y'^2}e^{-(y')^2(R')^{2h}/2}J_0(R')\ . \tag{3.7}$$

On the other hand, for smaller values of q, Eq. (3.5) shows that $\tilde{S}(q) \sim q^{-4}$. This is consistent with the fact that a self-affine surface always looks smooth on length scales $\gg R_0$,[28] where R_0 is defined in Eq. (2.7). Thus, we may write Eq. (3.4) as

$$\tilde{S}(q) \simeq A_1/q^4 + A_2/q^{3+h} , \qquad (3.8)$$

where

$$A_1/A_2 = c(R_0)^{1-h} , \qquad (3.9)$$

where c is a number of order unity.

Equation (3.8) was derived by Wong[24] for self-affine random surfaces using a completely different method. It is interesting to note that the orientational averaging yields a q^{-3-h} asymptotic form for $S(q)$ whereas a *single* surface yields as asymptotic form $q^{-2-(2/h)}$ for diffuse scattering with q normal to the surface.

A well-known special case arises when the surface is rough in a very special way corresponding to a self-similar fractal surface. We shall not discuss this case here as it has been discussed elsewhere.[23,24,28] Bale and Schmidt[23] were the first to show that for this case, the asymptotic form of $\tilde{S}(q) \sim q^{D_s-6}$, D_s being the fractal dimension of the surface. Both this form and $\tilde{S}(q)$ given in Eq. (3.4) yield an asymptotic power law in q with an exponent less than 4, the value for smooth surfaces. Thus, in practice it is difficult to distinguish self-affine from truly self-similar fractal surfaces. From Eq. (3.4) it may be seen that the limiting power laws are in fact consistent if we note the relation [Eq. (2.8)] between h and D_s. This has been already pointed out by Wong.[33]

An interesting question arises as to whether we can distinguish between a rough surface or interface and a graded interface, where there is a smooth and continuous decrease of scattering density normal to the interface (as at an interface where there is interdiffusion between the two media). The latter will yield an asymptotic $\tilde{S}(q)$ of the form $q^{-4}|f(q)|^2$, where $f(q)$ is an effective form factor for the scattering density $[\rho(z)]$ variations normal to the surface[3,17-20,34]

$$f(q) = \int_{-\infty}^{\infty} \left| \frac{d\rho(z)}{dz} \right| e^{-iqz} dz . \qquad (3.10)$$

This will in general cause the scattering at large q to fall *faster* than q^{-4}. On the other hand, *lateral roughness of a sharp interface* will cause the asymptotic form of the scattering to fall *slower* than q^{-4}.

IV. DISTORTED-WAVE BORN APPROXIMATION

We now attempt to go beyond the Born approximation, which will clearly break down when the reflectivity becomes nearly unity (near the critical angle for total external reflection), by using perturbation theory on the exact solution of the wave equation for a smooth surface. The distorted-wave born approximation[35] (DWBA) has been previously used by Vineyard[36] and others[37] in discussions of diffraction from surface structures. X rays polarized parallel to the average surface (TE polarization)

and neutrons, obey everywhere the stationary wave equation

$$\nabla^2 \psi + k_0^2 \psi - V\psi = 0 , \qquad (4.1)$$

where ψ is the wave function (for neutrons) or the electron-field parallel to the surface for x rays, k_0 is the magnitude of the wave vector in free space and

$$V = k_0^2(1-n^2) , \qquad (4.2)$$

where n is the refractive index given in Eq. (2.16). The case of TM polarized x rays is not discussed, since it is known that for grazing incidence it gives the same results as for TE polarization, because the refractive index differs from unity by only 1 part in $\sim 10^6$.

Let the plane $z = 0$ define the average smooth surface S_0 such that

$$\int \int_{S_0} dx \, dy \, z(x,y) = 0 . \qquad (4.3)$$

We write

$$V = V_1 + V_2 \qquad (4.4)$$

where

$$V_1 = \begin{cases} k_0^2(1-n^2), & -a < z < 0 \\ 0, & z > 0. \end{cases} \qquad (4.5)$$

(Since the matrix elements of V have to be bounded, we formally consider a slab $-a < z < 0$, rather than a semi-infinite medium, but if it is made thick enough, the difference can be made negligible.)

$$V_2 = \begin{cases} k_0^2(1-n^2) & \text{for } 0 < z < z(x,y) \text{ if } z(x,y) > 0 \\ -k_0^2(1-n^2) & \text{for } z(x,y) < z < 0 \text{ if } z(x,y) < 0 \\ 0 & \text{elsewhere,} \end{cases}$$

$$\qquad (4.6)$$

where $z(x,y)$ is the height of the actual surface at (x,y). V_2 is regarded as the perturbation on V_1 due to the roughness (see Fig. 4). We consider the surface to have
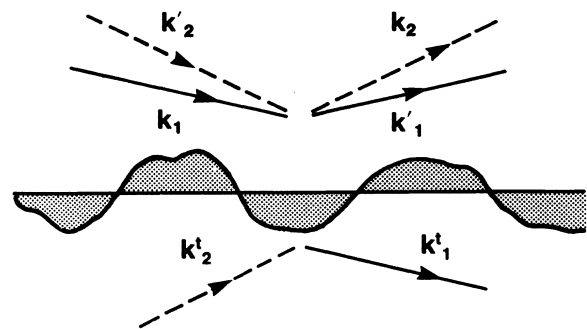

FIG. 4. Schematic of a rough surface. The horizontal line is the average surface ($z = 0$). The shaded regions are the regions of perturbation to a smooth surface. The incident wave vectors k_1 and $-k_2$, the reflected wave vectors $k_{1'}$ and $-k_{2'}$, and the transmitted wave vectors k_1^t and $-k_2^t$ are illustrated.

an extent L_x, L_y along the x,y directions with periodic boundary conditions. We assume that the volume is infinite in the z direction.

Consider a plane wave of wave vector $\mathbf{k}_1$ incident on the surface from $z > 0$. The Fresnel theory yields the exact eigenstate for the smooth surface ($V_2 = 0$) as

$$\psi_1(\mathbf{r}) = \begin{cases} C[e^{i\mathbf{k}_1 \cdot \mathbf{r}} + R(\mathbf{k}_1)e^{i\mathbf{k}_1' \cdot \mathbf{r}}], & z > 0 \\ CT(\mathbf{k}_1)e^{i\mathbf{k}_1^t \cdot \mathbf{r}}, & z < 0, \end{cases} \quad (4.7)$$

where $\mathbf{k}_{1'}$ is the wave vector of the specularly reflected beam and $\mathbf{k}_1^t$ that of the beam transmitted into the medium (see Fig. 4). C is a normalization constant chosen so that the beam has *unit incident flux*. R and T are the Fresnel reflection and transmission coefficients, respectively:

$$R(\mathbf{k}_1) = \frac{\sin\theta_1 - n \sin\theta_t}{\sin\theta_1 + n \sin\theta_t} , \quad (4.8a)$$

$$T(\mathbf{k}_1) = \frac{2 \sin\theta_1}{\sin\theta_1 + n \sin\theta_t} , \quad (4.8b)$$

where θ_1 is the *grazing* angle of incidence, θ_t is the corresponding *grazing* angle of refraction. Note that in general n and $\sin\theta_t$ can be complex. Snell's law states that

$$\cos\theta_t = \cos\theta_1/n . \quad (4.9)$$

The critical angle of incidence for total external reflection is given by $\theta_c = \cos^{-1}(n)$, thus, from Eq. (2.16)

$$\theta_c^2 = bN\lambda^2/\pi . \quad (4.10)$$

We also define another eigenstate for the smooth surface, which is a *time reversed state* for a beam incident on the surface with wave vector $-\mathbf{k}_2$

$$\tilde{\psi}_2(\mathbf{r}) = \begin{cases} C[e^{i\mathbf{k}_2 \cdot \mathbf{r}} + R^*(\mathbf{k}_2')e^{i\mathbf{k}_2' \cdot \mathbf{r}}], & z > 0 \\ CT^*(\mathbf{k}_1)e^{i\mathbf{k}_2^t \cdot \mathbf{r}}, & z < 0, \end{cases} \quad (4.11)$$

where $\mathbf{k}_2'$ is the incident wave vector which is specularly reflected as $\mathbf{k}_2$, and $\mathbf{k}_2^t$ is the wave vector in the medium which comes towards the surface and combines with wave $\mathbf{k}_2'$ to produce the time reversed wave $\mathbf{k}_2$. (We do not necessarily assume here that $\mathbf{k}_1$ and $\mathbf{k}_2$ are related by

specular reflection.) The DWBA can be written as an approximation for the T matrix for scattering between states $\mathbf{k}_1$ and $\mathbf{k}_2$,[35]

$$\langle 2 | T | 1 \rangle = \langle \tilde{\psi}_2 | V_1 | \phi_1 \rangle + \langle \tilde{\psi}_2 | V_2 | \psi_1 \rangle \quad (4.12)$$

where ϕ_1 is the *pure* incoming plane wave (again normalized to unit incident flux)

$$\phi_1(\mathbf{r}) = Ce^{i\mathbf{k}_1 \cdot \mathbf{r}} . \quad (4.13)$$

We assume some absorption in the medium (i.e., a small imaginary component to n) such that the first matrix element is finite when integrated over the semi-infinite medium. In such a case, it is easily shown that

$$\langle \tilde{\psi}_2 | V_1 | \phi_1 \rangle = | C |^2 2ik_0\sin\theta_1 R(\mathbf{k}_1)L_x L_y$$
$$\times \delta_{k_{1x},k_{2x}} \delta_{k_{1y},k_{2y}} \quad (4.14)$$

[where $\delta_{k_{1x},k_{2x}}$ implies a Kronecker delta in keeping with the periodic boundary conditions along (x,y) which keep k_{1x},k_{1y}, etc. as discrete quantized quantities for the moment].

The cross section is given in terms of $\langle 2 | T | 1 \rangle$ by

$$\frac{d\sigma}{d\Omega} = \frac{| \langle 2 | T | 1 \rangle |^2}{16\pi^2 | C |^4} . \quad (4.15)$$

Thus, if $V_2 = 0$, by Eq. (4.14)

$$\frac{d\sigma}{d\Omega} = \frac{1}{4\pi^2} k_0^2 \sin^2\theta_1 | R(\mathbf{k}_1) |^2 (L_x L_y)^2 \delta_{k_{1x},k_{2x}} \delta_{k_{1y},k_{2y}} . \quad (4.16)$$

As $L_x, L_y \to \infty$, we may switch to the delta-function representation

$$\delta_{k_{1x},k_{2x}} \to (2\pi/L_x)\delta(k_{2x} - k_{1x}), \text{ etc.,} \quad (4.17)$$

so that Eq. (4.16) may be written

$$\frac{d\sigma}{d\Omega} = (L_x L_y)k_0^2 \sin^2\theta_1 | R(k_1) |^2 \delta(q_x)\delta(q_y) , \quad (4.18)$$

where $\mathbf{q}$ is defined in Eq. (2.2). As in Sec. II, we see that this is simply the Fresnel specular reflection, expressed as a cross section, as may be seen by writing the reflectivity using Eqs. (2.13) and (2.14).

We now turn to an evaluation of the matrix element $\langle \tilde{\psi}_2 | V_2 | \psi_1 \rangle$ in Eq. (4.12). Using Eqs. (4.7) and (4.11) we obtain,

$$\langle \tilde{\psi}_2 | V_2 | \psi_1 \rangle = | C |^2 k_0^2 (1 - n^2)[F_>(q) + R(\mathbf{k}_2')F_>(\mathbf{q}_1) + R(\mathbf{k}_1)F_>(\mathbf{q}_2) + R(\mathbf{k}_2')R(\mathbf{k}_1)F_>(\mathbf{q}_3) + T(\mathbf{k}_2)T(\mathbf{k}_1)F_<(\mathbf{q}_t)] , \quad (4.19)$$

where

$$F_>(\kappa) = \int \int_{S_0} dx \, dy \int_0^{z(x,y) > 0} dz \, e^{-i\kappa \cdot \mathbf{r}}$$

$$= \frac{i}{\kappa_z} \int \int_{S_0 z(x,y) > 0} dx \, dy (e^{-i\kappa_z z(x,y)} - 1)e^{-i(\kappa_x x + \kappa_y y)} , \quad (4.20a)$$

$$F_<(\kappa) = \frac{i}{\kappa_z} \int \int_{S_0 \ z(x,y)<0} dx \ dy (e^{-i\kappa_z z(x,y)} - 1) e^{-i(\kappa_x x + \kappa_y y)} \ . \tag{4.20b}$$

In Eq. (4.19) the wave vectors are defined as follows:

$$\mathbf{q} = \mathbf{k}_2 - \mathbf{k}_1 \ ,$$

$$\mathbf{q}_1 = \mathbf{k}_2' - \mathbf{k}_1 = \mathbf{q} - \mathbf{k}_2 + \mathbf{k}_2' \ ,$$

$$\mathbf{q}_2 = \mathbf{k}_2 - \mathbf{k}_1' = \mathbf{q} - \mathbf{k}_1' + \mathbf{k}_1 \ , \tag{4.21}$$

$$\mathbf{q}_3 = \mathbf{k}_2' - \mathbf{k}_1' = \mathbf{q} - \mathbf{k}_1' + \mathbf{k}_1 - \mathbf{k}_2 + \mathbf{k}_2' \ ,$$

$$\mathbf{q}_t = \mathbf{k}_2^t - \mathbf{k}_1^t \ ,$$

$\mathbf{q}_t$ is the wave-vector transfer *in* the medium. For specular reflection with $\theta_1 < \theta_c$, $\mathbf{q}_t$ is essentially purely imaginary. It is zero at $\theta = \theta_c$ and increases with a small imaginary component (corresponding to attenuation) beyond θ_c. For $\theta \gg \theta_c$, $\mathbf{q}$ and $\mathbf{q}_t$ are essentially equal. Note that by the definitions of these vectors

$$q_{(x,y)} = q_{1(x,y)} = q_{2(x,y)} = q_{3(x,y)} = q_{t(x,y)}$$

$$(\ = 0 \text{ at specular}) \ , \tag{4.22}$$

$$q_{2z} = -q_{1z} \ (\ = 0 \text{ at specular}), \quad q_{3z} = -q_z \ .$$

Equations (4.14) and (4.19) have to be summed and substituted in Eq. (4.15) and finally a configurational average over the random rough surface has to be carried out. In evaluating this average, we use the result that if B

is a fluctuating quantity,

$$\langle |A + B|^2 \rangle = |A + \langle B \rangle|^2 + \{ \langle BB^* \rangle - |\langle B \rangle|^2 \} \ . \tag{4.23}$$

The first term on the right yields the specular reflection, and the second term yields the diffuse scattering. We need to evaluate the quantities $\langle F_>(\kappa) \rangle$ and $\langle F_<(\kappa) \rangle$ to obtain the specular term. We define $w(z)$ to be the height distribution of the surface, with the average surface $(z = 0)$ chosen such that

$$\int_0^\infty dz \ w(z) = \int_{-\infty}^0 dz \ w(z) = \tfrac{1}{2} \ . \tag{4.24}$$

For a Gaussian random surface

$$w(z) = \frac{e^{-z^2/2\sigma^2}}{\sigma(2\pi)^{1/2}} \ . \tag{4.25}$$

We note that in general, $w(z)$ need not be symmetric in z. If one is only interested in weak specular scattering from a rough surface, or the case of a smooth but graded interface, $w(z)$ can be written in terms of the average density:

$$w(z) = \frac{d\bar\rho(z)}{dz} \frac{1}{\rho_{\text{bulk}}} \ . \tag{4.26}$$

Using Eq. (4.20) we can now write

$$\langle F_>(\kappa) \rangle = \frac{i}{\kappa_z} \int \int_{S_0} dx \ dy \int_0^\infty dz \ w(z)(e^{-i\kappa_z z} - 1) e^{-i(\kappa_x x + \kappa_y y)} = \frac{i}{\kappa_z} L_x L_y \delta_{\kappa_x,0} \delta_{\kappa_y,0} [W_>(\kappa) - \tfrac{1}{2}] \ ,$$

$$\langle F_<(\kappa) \rangle = \frac{i}{\kappa_z} L_x L_y \delta_{\kappa_x,0} \delta_{\kappa_y,0} [W_<(\kappa) - \tfrac{1}{2}] \ , \tag{4.27}$$

where

$$W_>(\kappa) \equiv \int_0^\infty dz \ w(z) e^{-i\kappa_z z} \quad \text{and} \quad W_<(\kappa) \equiv \int_{-\infty}^0 dz \ w(z) e^{-i\kappa_z z} \ .$$

For the case when $z(x,y)$ is a Gaussian random variable with standard deviation σ, we can write

$$\langle F_>(\kappa) \rangle = \frac{i}{\kappa_z} (L_x L_y) \delta_{\kappa_x,0} \delta_{\kappa_y,0} \{ \tfrac{1}{2} [e^{-\kappa_z^2 \sigma^2/2} - 1] - i\kappa_z \sigma \mathcal{F}(\kappa_z^2 \sigma^2) \} \ ,$$

$$\langle F_<(\kappa) \rangle = \frac{i}{\kappa_z} (L_x L_y) \delta_{\kappa_x,0} \delta_{\kappa_y,0} \{ \tfrac{1}{2} [e^{-\kappa_z^2 \sigma^2/2} - 1] + i\kappa_z \sigma \mathcal{F}(\kappa_z^2 \sigma^2) \} \ , \tag{4.28}$$

where

$$\mathcal{F}(x) = \frac{1}{(2\pi)^{1/2}} \sum_{k=1}^\infty \frac{1}{(2k-1)!!} (-x)^{k-1} \ .$$

The Kronecker deltas yield the specular condition as before, we note that at specular, by the definitions of Eq. (4.21), $q_1 = q_2 = 0$ and $q_3 = -q$, so that

$$\langle F_{\gtrless}(\kappa) \rangle = \langle F_{\gtrless}(-\kappa) \rangle^* \ . \tag{4.29}$$

Substituting in Eq. (4.15), we finally obtain

$$\left[\frac{d\sigma}{d\Omega}(k_1,k_2)\right]_{\text{spec}} = \frac{(L_xL_y)^2}{16\pi^2}\delta_{k_{1x},k_{2x}}\delta_{k_{1y},k_{2y}}\left|2k_0\sin\theta_1 R(\mathbf{k}_1)\right.$$

$$-\frac{q_c^2}{4}\left[\frac{1}{2q_z}(1-e^{-q_z^2\sigma^2/2})[1-R^2(\mathbf{k}_1)]+\frac{1}{2q_z^t}(1-e^{-(q_z^t)^2\sigma^2/2})T^2(\mathbf{k}_1)\right.$$

$$\left.\left.+\frac{i2\sigma R(\mathbf{k}_1)}{(2\pi)^{1/2}}+i\sigma\{\mathcal{F}(q_z^2\sigma^2)[1+R^2(\mathbf{k}_1)]-\mathcal{F}((q_z^t)^2\sigma^2)T^2(\mathbf{k}_1)\}\right]\right|^2,$$

$$(4.30)$$

where we have defined

$$q_c^2 \equiv 4k_0^2(1-n^2) . \tag{4.31}$$

(q_c corresponds to q_z at the critical angle θ_c at specular reflection.) If we recognize that at specular $q_z=2k_0\sin\theta_1$ and use the delta-function representation, Eq. (4.30) can be slightly simplified to yield

$$\frac{d\sigma}{d\Omega}(k_1,k_2)=(L_xL_y)\delta(q_x)\delta(q_y)k_0^2\sin^2\theta_1|\tilde{R}(k_1)|^2 \tag{4.32}$$

which is to be compared with Eq. (4.18) for the smooth surface. The specular reflectivity for the rough surface is now given by

$$\tilde{R}(\mathbf{k}_1)=R(\mathbf{k}_1)-\frac{q_c^2}{4}\left[\frac{1}{2q_z^2}(1-e^{-q_z^2\sigma^2/2})[1-R^2(\mathbf{k}_1)]+\frac{T^2(\mathbf{k}_1)}{2q_zq_z^t}(1-e^{-(q_z^t)^2\sigma^2/2})\right.$$

$$\left.+\frac{i2\sigma R(\mathbf{k}_1)}{(2\pi)^{1/2}q_z}+\frac{i\sigma}{q_z}\{\mathcal{F}(q_z^2\sigma^2)[1+R^2(\mathbf{k}_1)]-\mathcal{F}((q_z^t)^2\sigma^2)T^2(\mathbf{k}_1)\}\right] . \tag{4.33}$$

Note that $\tilde{R}(\mathbf{k}_1)$ depends only on the optical constants and on σ. Expanding the Gaussians in Eq. (4.33) for small values of $\mathbf{q}_t$ and $\mathbf{q}$, and using identities relating R, T^2, q_z, and q_z^t, we obtain a result consistent with

$$|\tilde{R}(\mathbf{k}_1)|^2 = |R(\mathbf{k}_1)|^2 e^{-q_zq_z^t\sigma^2} \quad (q_z \geq q_c) \tag{4.34}$$

to order q_z^2, assuming that $q_c\sigma$ is not large. This has been obtained previously by Nevot and Croce using a different method.[21] Figure 5 compares calculations using the Born approximation [Eq. (2.28a)], the DWBA [Eq. (4.33)] and the "qq_t" expansion [Eq. (4.34)], for $\sigma=8$ Å.

We can see that for $q_z\sigma \leq 1$, the DWBA [Eq. (4.33)] and Eq. (4.34) agree well as they should, but the Born approximation [Eq. (2.28a)] is clearly wrong, as it diverges instead of saturating at total reflection. On the other hand, for $q_z\sigma \gg 1$, Eq. (4.34) and the Born approximation agree very well, while the DWBA [Eq. (4.33)] yields too large a value for the specular reflectivity. This is because the Fresnel eigenstates, which form the basis states for the perturbation theory, are in this regime very far from being a good approximation to the eigenstates of the system. In this case, however, the Born approximation is satisfactory, and being far away from the critical angle, Eq. (4.34) is equivalent. Thus, if would appear that Eq. (4.34) is a good crossover form, which matches both the DWBA and the Born approximation in their respective regimes of validity.

Secondly, a rough surface should yield for $q_z<q_c$ $|R|^2<1$ due to scattering losses, as is seen experimentally, whereas the DWBA does not correctly show this.

This is because the scattering is at the unitarity limit and one should employ the second-order Born approximation in this regime: Basically a manifestation of the fact that the optical theorem is not satisfied by the first order Born approximation.[38] On the other hand, for $q_z\sigma \leq 1$, in this limit one may go systematically beyond the first-order Born approximation using methods given (primarily for treating the case of visible light reflecting from rough surfaces) by Brown et al.[39] and Toigo et al.[40] In most of
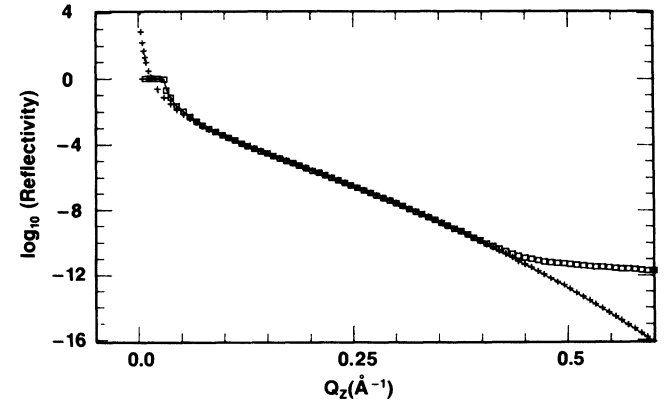

FIG. 5. The computed reflectivity of Pyrex at $\lambda=1.46$ Å with $\sigma=8$ Å, using the Born approximation (crosses), the DWBA (open squares), and the form given by Eq. (4.34) (solid line).

these treatments, however, the exponential involving $\kappa_z z(x,y)$ in the matrix elements of Eq. (4.20) is expanded in terms of $\kappa_z z(x,y)$, leading to expressions involving the Fourier transform of the height-height correlation function directly, whereas (as we later show) this is only accurate near the critical angle. Thus, these treatments would not be accurate for large q_z. Since the reflectivity for large q_z is weak, the form given here, which uses the Born approximation, but does not expand the exponential would be expected to be more accurate in that regime. We may summarize the situation in the following way: For $q_z \sigma \geq 1$, Eq. (4.34), which represents a good interpolation between the DWBA and the Born approximation forms given here, is a good approximation to the specular reflectivity. For $q_z \leq q_c$ when $q_c \sigma \geq 1$, an accurate calculation of the reflectivity involves higher-order Born approximations as discussed in Refs. 39 and 40 and the

form given here [Eq. (4.33) or (4.44)] is less accurate.

One sometimes considers graded, but smooth interfaces, where the density is only a function of z. In such cases, there is no diffuse scattering and one may obtain a result of the desired degree of accuracy by employing the "matrix method[41-43]" where the interface is divided into many uniform thin slabs, which can each be treated exactly. One may reduce a rough surface to a graded interface. However, diffuse scattering information is lost. In the weak scattering limit, the specular is unaffected by such an approximation, but in the unitarity scattering limit, while an exact solution is provided for the graded interface, it is not valid for a rough surface.[18]

We expand the case of a general $w(z)$ for small $q_z \sigma$ $[W(q_z) \simeq W^*(q_z)]$, the imaginary terms which effect the scattering only to second order can be neglected and thus,

$$\int_0^\infty dz\, w(z) e^{-iq_z z} \approx \tfrac{1}{2} - \int_0^\infty dz \frac{w(z)}{2} q_z^2 z^2 \ , \tag{4.35}$$

$$\tilde{R} = R \left[1 - (1 - q_c^2/q_z^2)^{1/2} q_z^2 \int_0^\infty dz \frac{w(z)}{2} z^2 - (1 - q_c/q_z)^{-1/2} (q_z')^2 \int_{-\infty}^0 dz \frac{w(z)}{2} z^2 \right]$$

$$\approx R \left[1 - q_z q_z' \int_{-\infty}^\infty dz \frac{w(z)}{2} z^2 \right] \tag{4.36}$$

$$|\tilde{R}|^2 \approx \left| R \int_{-\infty}^\infty dz\, w(z) e^{-i\sqrt{q_z q_z'} z} \right|^2 \ . $$

We only derived the above expression for small q values, however for large q_z, where $q_z' \to q_z$, this is the result in the Born approximation[3,17-20,34] and thus, is the generalization of Eq. (4.34), which is valid in both limits.

Using averages of the following form:

$$\langle F_>(\kappa) F_>^*(\kappa) \rangle = \frac{1}{\kappa_z^2} \int \int_{S_0} dx\, dy \int \int_{S_0} dx'\, dy' \langle (e^{-i\kappa_z z(x,y)} - 1)(e^{i\kappa_z z(x',y')} - 1) \rangle \exp\{ -i[\kappa_x(x-x') + \kappa_y(y-y')] \} \ , \tag{4.37}$$

$$\langle F_>(\kappa_1) F_<(\kappa_2) \rangle = 0 \ , $$

the diffuse scattering can be calculated from the second term in Eq. (4.23), resulting in a complicated expression which may be considerably simplified by making the following approximation: We assume that even for $z > 0$, but inside the actual surface, we may approximate $\psi_1(\mathbf{r})$ and $\psi_2(\mathbf{r})$ by their expressions for $z < 0$ [Eqs. (4.7) and (4.11)]. Since the wave function and its derivative have to be continuous at $z = 0$, such an approximation is reasonable for $q_z \sigma \ll 1$, which is the only regime where we need to go beyond the Born approximation to calculate the diffuse scattering. Thus,

$$\langle \tilde{\psi}_2 | V_2 | \psi_1 \rangle \simeq |C|^2 T(\mathbf{k}_1) T(\mathbf{k}_2) k_0^2 (1 - n^2) F(\mathbf{q}_t) \ , \tag{4.38}$$

where

$$F(\mathbf{q}_t) = \frac{i}{q_z'} \int \int_{S_0} dx\, dy (e^{-iq_z' z(x,y)} - 1) e^{-i(q_x x + q_y y)} \ . \tag{4.39}$$

If we carry out the configurational average, we obtain

$$|\langle \tilde{\psi}_2 | V_2 | \psi_1 \rangle|^2 = |C|^4 |T(\mathbf{k}_1)|^2 |T(\mathbf{k}_2)|^2 |k_0^2 (1 - n^2)|^2 [\langle F(\mathbf{q}_t) F^*(\mathbf{q}_t) \rangle - \langle F(\mathbf{q}_t) \rangle \langle F^*(\mathbf{q}_t) \rangle] \ . \tag{4.40}$$

This may be evaluated to yield for the diffuse cross section

$$\left[\frac{d\sigma}{d\Omega} \right]_{\text{diff}} = (L_x L_y) \frac{|k_0^2 (1 - n^2)|^2}{16\pi^2} |T(\mathbf{k}_1)|^2 |T(\mathbf{k}_2)|^2 S(\mathbf{q}_t) \ , \tag{4.41}$$

where

$$S(\mathbf{q}_t) = \frac{\exp\{-[(q_z^t)^2 + (q_z^{t*})^2]\sigma^2/2\}}{|q_z^t|^2} \int \int_{S_0} dX\, dY (e^{|q_z^t|^2 C(X,Y)} - 1) e^{i(q_x X + q_y Y)}. \tag{4.42}$$

Comparison with Eq. (2.26) shows that Eq. (4.41) is identical with the expression for the scattering in the Born approximation except for (a) the factors $|T(\mathbf{k}_1)|^2 |T(\mathbf{k}_2)|^2$, (b) the use of q_z^t instead of q_z, and (c) the term (-1) inside the integrand of Eq. (4.42). This latter term simply subtracts off a specular part of the scattering which was not explicitly separated in Eq. (2.26). Thus, the diffuse scattering in the DWBA is easily evaluated using $T(\mathbf{k})$ from the Fresnel theory. For large q_z, $|T|^2 \simeq 1$ and $q_z^t \simeq q_z$ so Eq. (4.41) reduces to the Born approximation as it should. An interesting effect, however arises when $\mathbf{k}_1$ or $\mathbf{k}_2$ makes an angle close to θ_c with the surface; since $|T(\mathbf{k}_1)|^2$ or $|T(\mathbf{k}_2)|^2$ then has a maximum. The result is that a transverse scan (along q_x say) will have peaks in the diffuse scattering[25] (known as "Yoneda scattering," "anomalous reflections," or "angel's wings") whenever θ_1 or θ_2 is equal to θ_c. This is illustrated by a calculation shown in Fig. 6, which is the same calculation for Fig. 2, but now in the DWBA. The physical origin is the fact that when θ_1 or $\theta_2 = \theta_c$, the electric field at the surface reaches a maximum of twice the incident field, resulting in greater diffuse scattering. The symmetry of Eq. (4.41) with respect to $\mathbf{k}_1$ and $\mathbf{k}_2$ is a manifestation of microscopic reversibility and the reciprocity principle.[44,45]

An interesting consequence of Eq. (4.42) is that when q_z^t is very small, we may expand the exponential in Eq. (4.42) to obtain

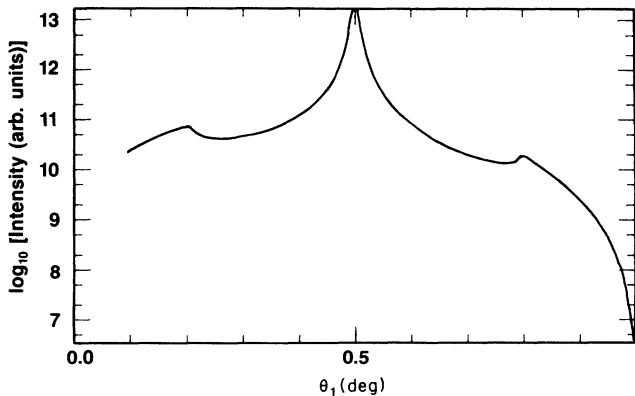$$S(\mathbf{q}_t) \simeq \int \int_{S_0} dX\, dY\, C(X,Y) e^{i(q_x X + q_y Y)}, \tag{4.43}$$

FIG. 6. Calculation of diffuse scattering in the distorted-wave Born approximation for rocking curve where θ_1 and θ_2 are varied such that 2θ is fixed at 1°. The asymmetry is due to the area of the illuminated surface decreasing as θ_1 is increased. The q_y direction has been integrated over. Parameters are $\sigma = 7$ Å, $h = 0.2$, $\xi = 7000$ Å, and the optical constants for Pyrex are given in Sec. V.

i.e., for a transverse scan (where $q_z \sigma \ll 1$), the diffuse scattering *directly yields the Fourier transform of the height-height correlation function of the surface.* This is *not* true in general, as has sometimes been assumed.

V. COMPARISON WITH EXPERIMENT

For an experiment done with an incident beam of fixed width and intensity I_0, and where the detector subtends a solid angle $\Delta\Omega$ at the sample, the intensity I scattered into the detector is given as follows: For specular, where the detector automatically integrates over the $\delta(q_x)\delta(q_y)$ factors in the cross section, as discussed in Sec. II,

$$I_{\text{spec}} = I_0 |\tilde{R}|^2 \tag{5.1}$$

while for the diffuse scattering,

$$I_{\text{diff}} = I_0 \frac{\Delta\Omega}{A} \left[\frac{d\sigma}{d\Omega} \right]_{\text{diff}}, \tag{5.2}$$

where A is the area of the beam.

We now present x-ray data taken on a rough piece of polished glass and show how the scattering can be analyzed in terms of the above formalism. The Pyrex glass, obtained from Melles Griot, is 50 mm × 50 mm and 10 mm thick, and was polished to be optically flat to $\lambda/10$ ($\lambda = 5460$ Å). Since figure error can make such an experiment difficult, it is important to find a surface which is macroscopically flat. We measured no observable figure error, down to 0.0025°. While the character of the surface of this polished glass is not especially interesting in and of itself, as its roughness is not expected to follow any fundamental or simple form, we present the data to show how such measurements can be used to study the character of roughness. It is also of interest since this and similar substrates are currently being used for deposition and wetting experiments on amorphous surfaces.

The experiment was carried out at the National Synchrotron Light Source (NSLS), Exxon beam-line X10A, which is on a bending magnet and has a focussing mirror (at 11 m) midway between the source and the sample (22 m). The beam was defined in the vertical direction using a double crystal Si(111) monochromator which selected $\lambda = 1.46$ Å. For Pyrex $(1 - n = 6.3 \times 10^{-6} + i8.5 \times 10^{-8})$ which gives a critical angle of $\theta_c = 0.20°$. The vertical width of the beam was 0.1 mm. which in principle allowed us to measure down to $\theta_1 = 0.12°$ with the entire beam hitting the sample. Below that angle, only a portion of the beam intersects the sample. This can be corrected for, by measuring the amount transmitted with the detector in the direct beam at $2\theta = 0°$ and rocking the sample. Such corrections are tricky and the data can be complicated if the edge of the sample is not perfectly smooth. Our analysis is concerned primarily with the

weak scattering regime and so the details of the scattering associated with the critical angle are not concentrated on here. The incident beam was defined in the out-of-plane (horizontal) direction by slits, and was 0.2 mm wide at the sample with an incident divergence of $\sim 0.06°$.

Two analyzer configurations were used: We used a triple-bounce Si(111) analyzer crystal in the dispersive geometry (which becomes nondispersive on reflection), which gave a profile in the main beam with FWHM of $0.0025°$ to put an upper limit on the figure error of the surface and also to confirm existence of separate specular ("delta function") and diffuse peaks at that resolution. For most of the measurements, no analyzer crystal was used. Instead, we used a pair of slits 0.8 mm wide, 960 mm from the sample, giving us a main beam profile with FWHM of $0.05°$. The out-of-plane slits after the sample were effectively left open, so the diffuse scattering was integrated over one direction parallel to the surface. We found that the lower resolution setup was advantageous for two reasons. Firstly, because we were interested in

measuring diffuse scattering, the scattered intensity was proportional to the resolution width. Secondly, we found that both the mosaic of the sample and the angular resolution were better than the reproducible stepsize of the spectrometer. Thus, lower resolution insured being able to obtain the full peak intensity of the specular component.

To measure the scattering along q_z, scans were performed under the specular condition $\theta_1 = \theta_2$ and also under the condition where $\theta_1 = \theta_2 \pm c$ where c is a small constant (usually $0.03°$) but large enough so that none of the delta-function specular scattering was encountered. This yielded a measure of the diffuse scattering intensity near $q_x = 0$ as a function of q_z. The specular to diffuse ratio was 135 at $2\theta = 1°$, 30 at $2\theta = 2°$, and 3.5 at $2\theta = 4°$. Rocking scans were done at constant values of $2\theta = \theta_1 + \theta_2$ which are essentially equivalent to q_x scans at constant q_z. Dark counts were subtracted from the data and the background, both measured with no sample, and the base line of transverse scans was found to be negligible.
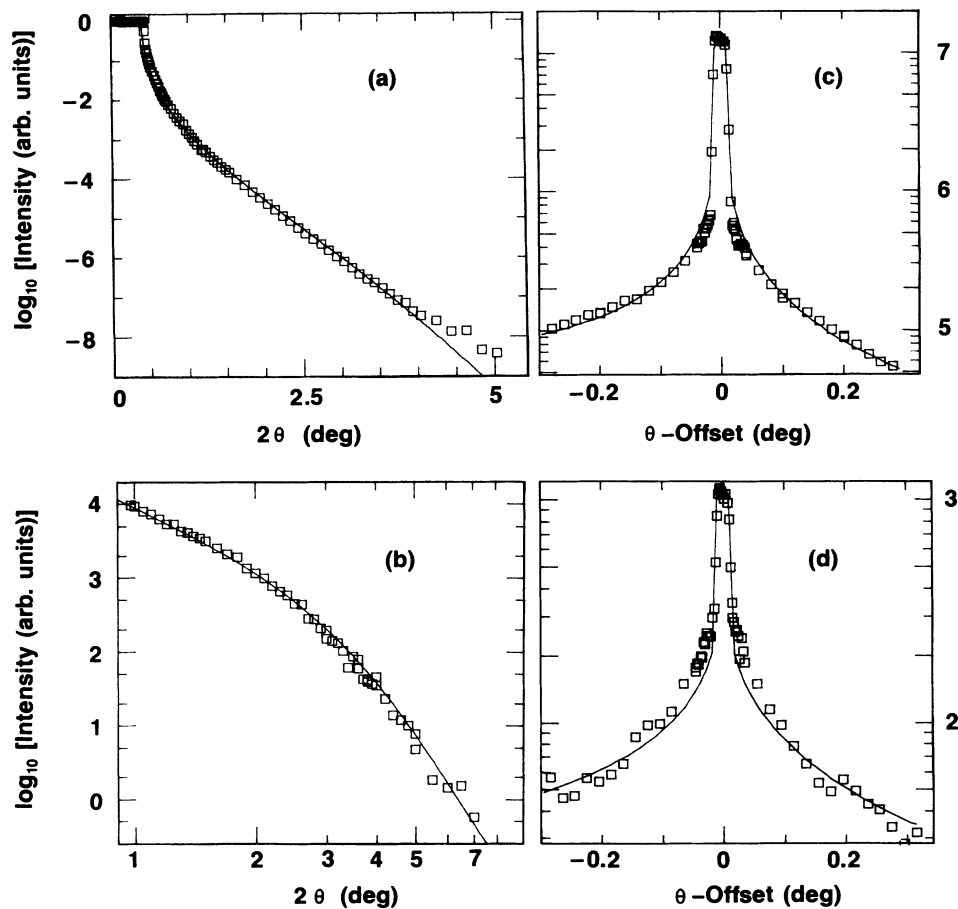

FIG. 7. Measured x-ray intensity vs angle for polished Pyrex surface. Data is represented by squares and fits by solid lines. Statistical errors are approximately the size of the squares. Intensities are on arbitrary logarithmic scales. Fits yielded the parameters $\sigma = 7.6$ Å, $\xi = 7000$ Å, and $h = 0.2$. (a) Specular reflection with diffuse subtracted out. (b) Diffuse scattering near specular $\theta_1 = \theta_2 + 0.03°$. ($2\theta$ is a log scale.) (c),(d) Transverse (rocking) scans; diffuse and specular are convolved with resolution. Intensity vs θ offset ($\theta_1 - \theta_2$) at (c) $2\theta = 2°$ and (d) $2\theta = 4°$. The systematic discrepancies between the fits and the data show that the roughness of this polished glass is not exactly given by the simple expression used.

The specular, diffuse-near-specular $(\theta_1 = \theta_2 + c)$ and transverse scans shown in Fig. 7, were fit self-consistently and convoluted with the resolution function, using the forms in Eqs. (4.34), (4.41), and (2.9), for a Gaussian surface whose roughness is power law with a cutoff. To get a correct measure of the diffuse scattering appearing in the specular scan it is necessary to extrapolate the diffuse near specular measured at finite q_x to $q_x = 0$ using the transverse lineshapes. (The high-resolution scans showed that it was not singular.) In practice, this did not significantly affect the results for the rms roughness determined to be $\sigma = 7.6 \pm 0.2$ Å. The diffuse-near-specular scan was most sensitive to the exponent $h = 0.2 \pm 0.02$ and the transverse scans were sensitive to the cutoff $\zeta = 7000 \pm 1000$ Å. The overall falloff of the specular appeared to be nearly Gaussian over ≥ 7 orders of magnitude, but began to diverge at larger angles, implying that $w(z)$ is not exactly Gaussian. The diffuse longitudinal scan fits surprisingly well. The data for the transverse scans does not fit extremely well. However, this is not unexpected since that scan would be sensitive to the precise form of the roughness, and we do not expect such a piece of polished glass to have a very simple spectral density of roughness.

VI. CONCLUSION

We have discussed the scattering of x rays and neutrons from rough surfaces in both the Born approximation and the distorted-wave Born approximation. The expression for the specular reflectivity given by the latter agrees well with the expression given by Nevot and Croce[21] provided $q_z \sigma \leq 1$, whereas the Born approximation is valid for $q_z \sigma \gg 1$. Below the critical angle for total external reflection, none of the approximations can account for reflectivities below unity, caused by losses due to diffuse scattering. We have also derived an expression for the specular reflectivity for an arbitrary graded interface in the distorted-wave Born approximation.

The importance of the diffuse scattering has also been emphasized and expressions for the latter were given in both the Born and distorted-wave Born approximations. Explicit expressions have been given for the case where the surface can be represented as a self-affine random Gaussian surface, since it is known[27] that such surfaces can represent real physical solid surfaces rather well. We also evaluated the case of liquid surfaces where the surface mean-square height fluctuations diverge logarithmically. We introduced finite length cutoffs in the case of both self-affine and liquid surfaces, and showed that such cutoffs lead to the reemergence of the specular reflections. It is hoped that the expressions given here may be useful in analyzing the results from real solid and liquid surfaces and obtaining information regarding the height-height correlation functions of such surfaces. For the present, we have illustrated the applicability of the formalism by studying the diffuse scattering and specular reflection from an optically polished Pyrex glass surface and modelling the scattering in terms of a self-affine surface with a finite cutoff. This amounts simply to a mathematical description of the surface inferred from the scattering. Of greater interest may be future experiments on surfaces or interfaces produced by sputtering, evaporation or other growth processes where simple physical predictions can be tested. We note in passing that high-resolution diffuse scattering experiments on surfaces of extreme flatness offer the possibility of examining roughness characteristics to length scales of the order of microns.

By averaging over random orientations, we have discussed the connection of these results to those already well known in the theory of small-angle scattering from materials with large internal surfaces, including the well known asymptotic power-law forms for $S(q)$. It is also easy to show that, at least in the Born approximation, the method can be used to discuss scattering at and near truncation rods[46] from crystalline surfaces. This is because the density of a crystalline solid can be written as

$$\rho(r) = \rho_0(r) \sum_i \delta(r - r_i) , \qquad (6.1)$$

where $\rho_0(r)$ is the density of a *uniform* solid possessing the rough surface and r_i are the atomic positions of an *infinite* crystal lattice. Scattering in the Born approximation then yields that the diffuse scattering *due to surface roughness* at wave-vector transfer $\mathbf{Q}$ is given by

$$S_{\text{cryst}}(\mathbf{Q}) = \sum_{\mathbf{G}} S_{\text{diff}}(\mathbf{Q} - \mathbf{G}) , \qquad (6.2)$$

where $\mathbf{G}$ is a reciprocal lattice vector and $S_{\text{diff}}(\mathbf{q})$ is the result obtained above [Eq. (2.28b)]. We have assumed that the structure factor of the infinite crystal is a series of delta functions at the reciprocal lattice vectors and neglected thermal Debye-Waller effects. Thus, the scattering derived in this paper for small q will be replicated at all $\mathbf{Q} = \mathbf{G} + \mathbf{q}$, and will be apparent at $\mathbf{Q}$ values where the scattering from the bulk is small. The "specular ridge" $(q_x = q_y = 0)$ is now reflected in rods emanating from all $\mathbf{G}$ vectors in reciprocal space normal to the physical crystal surface (the so-called "truncation rods"). This is consistent with the results derived by slightly different methods.[46] Of course, if the roughness is *highly correlated with the atomic arrangements* (e.g., in the form of steps[47]) then Eq. (6.1) is invalid and the scattering must be discussed separately from the case discussed here.

*Present address: Department of Physics, Carnegie Mellon University, Pittsburgh, PA 15213.

†Present address: Imperial Chemical Industries, The Heath, Runcorn, Cheshire, England.

[1]L. G. Parratt, Phys. Rev. 95, 359 (1954).

[2]J. O. Porteus, J. Opt. Soc. Am. 53, 1394 (1963).

[3]A. Braslau, M. Deutsch, P. S. Pershan, A. H. Weiss, J. Als-Nielsen, and J. Bohr, Phys. Rev. Lett. 54, 114 (1985).

[4]M. V. Zombeck, C. C. Wyman, and M. C. Weisskopf, Proc. Soc. Photo-Opt. Instrum. Eng. 257, 230 (1980).

[5]L. A. Smirnov, T. D. Sotnikova, and Yu. I. Kogan, Opt. Spectrosc. (USSR), 58, 239 (1985); L. A. Smirnov and S. B. Anokhin, ibid. 48, 315 (1980); L. A. Smirnov, ibid. 48, 629 (1980); L. A. Smirnov, T. D. Sotnikova, B. S. Anokhin, and B. Z. Taibin, ibid. 46, 329 (1979).

[6]J. M. Elson, Phys. Rev. B 30, 5460 (1984); J. M. Elson and J. M. Bennett, Opt. Eng. 18, 116 (1979); J. M. Elson, J. P. Rahn, and J. M. Bennett, Appl. Opt. 19, 669 (1980); J. M. Bennett, ibid. 11, 2075 (1976).

[7]P. Beckmann and A. Spizzichino, The Scattering of Electromagnetic Waves From Rough Surfaces (Pergamon, New York, 1963).

[8]A. V. Vinogradov, N. N. Zorev, I. V. Kozhevnikov, and I. G. Yakushkin, Zh. Eksp. Teor. Fiz. 89, 2124 (1985) [Sov. Phys.—JETP 62, 1225 (1985)].

[9]P. A. J. de Korte and R. Laine, Appl. Opt. 18, 236 (1979).

[10]E. A. Stewardson and J. H. Underwood, Br. J. Appl. Phys. 16, 1877 (1965).

[11]J. M. Elson, V. Rehn, J. M. Bennett, and V. O. Jones, Proc. Soc. Photo-Opt. Instrum. Eng. 315, 193 (1981); V. Rehn, Low Energy X-Ray Diagnostics-1981 (Monterey, California), Proceedings of the Topical Conference on Low Energy X-Ray Diagnostics, AIP Conf. Proc. No. 75, edited by David T. Attwood and Burton L. Henke (AIP, New York, 1981); V. Rehn, V. O. Jones, J. M. Elson, and J. M. Bennett, Nucl. Instrum. Meth. 172, 307 (1980).

[12]P. Eisenberger and A. Y. Cho, J. Appl. Phys. 50, 6927 (1979).

[13]H. E. Bennett and J. O. Porteus, J. Opt. Soc. Am. 51, 123 (1961).

[14]K. Lindsley, in Proceedings of the X-Ray Optics Symposium, edited by P. W. Stanford (Science Research Council, London, 1974); E. L. Church, J. A. Jenkinson, and J. M. Zavada, Opt. Eng. 16, 360 (1977); 18, 125 (1979); E. L. Church, Proc. Soc. Photo-Opt. Instrum. Eng. 184, 196 (1979).

[15]D. W. Oxtoby, F. Novak, and S. A. Rice, J. Chem. Phys. 76, 5278 (1982).

[16]G. P. Felcher, J. R. Penfold, and R. K. Thomas (private communication).

[17]E. S. Wu and W. W. Webb, Phys. Rev. A 8, 2065 (1973).

[18]J. Meunier and D. Langevin, J. Phys. (Paris) Lett. 43, L185 (1982).

[19]P. S. Pershan, A. Braslau, A. H. Weiss, and J. Als-Nielsen, Phys. Rev. A 35, 4800 (1987).

[20]J. Meunier, C. R. Acad. Sc. Paris Ser. B. 292, 1469 (1981).

[21]L. Nevot and P. Croce, Rev. Phys. Appl. 15, 761 (1980).

[22]Small Angle X-Ray Scattering, edited by O. Glatter, and O. Kratky (Academic, New York, 1982) and references therein.

[23]H. D. Bale and P. W. Schmidt, Phys. Rev. Lett. 53, 596 (1984).

[24]P. Z. Wong, Phys. Rev. B 32, 7417 (1985).

[25]Y. Yoneda, Phys. Rev. 131, 2010 (1963); O. J. Guentert, J. Appl. Phys. 30, 1361 (1965); A. N. Nigam, Phys. Rev. A 4, 1189 (1965).

[26]B. B. Mandelbrodt, The Fractal Geometry of Nature (Freeman, New York, 1982).

[27]R. F. Voss, in Fundamental Algorithims for Computer Graphics, edited by R. A. Earnshaw (Springer-Verlag, Berlin, 1985), p. 808; R. F. Voss, in Scaling Phenomena in Disordered Systems, edited by R. Pynn and A. Skjeltorp (Plenum, New York, 1985), p. 1.

[28]S. Alexander, in Transport and Relaxation in Random Materials, edited by J. Klafter, R. Rubin, and M. F. Schlesinger (World-Scientific, Singapore, 1987).

[29]D. Sluis and S. A. Rice, J. Chem. Phys. 79, 5658 (1983).

[30]L. D. Landau and E. M. Lifshitz, Fluid Mechanics (Pergamon, Oxford, 1986), p. 237.

[31]P. Dutta and S. K. Sinha, Phys. Rev. Lett. 47, 50 (1981).

[32]Handbook of Mathematical Functions, edited by M. Abramowitz and I. A. Stegun (National Bureau of Standards, Washington, 1972).

[33]P.-z. Wong (unpublished).

[34]B. M. Ocko, P. S. Pershan, C. R. Safinya, and L. Y. Chiang, Phys. Rev. A 35, 1868 (1987); P. S. Pershan, J. Als-Nielsen, Phys. Rev. Lett. 52, 759 (1984); J. Als-Nielsen, F. Christensen, and P. S. Pershan, ibid. 48, 1107 (1982).

[35]L. I. Schiff, Quantum Mechanics (McGraw-Hill, New York, 1968).

[36]G. H. Vineyard, Phys. Rev. B 50, 4146 (1982).

[37]U. Mohanty and S. A. Rice, J. Chem. Phys. 79, 2482 (1983).

[38]J. D. Jackson, Classical Electrodynamics (Wiley, New York, 1975), pp. 453–459.

[39]G. Brown, V. Celli, M. Haller, A. A. Maradudin, and A. Marvin, Phys. Rev. B 31, 4993 (1985).

[40]F. Toigo, A. Marvin, V. Celli, and N. R. Hill, Phys. Rev. B 15, 5618 (1977).

[41]M. Born and E. Wolf, Principles of Optics (Pergamon, New York, 1980).

[42]B. N. Thomas, S. W. Barton, F. Novak, and S. A. Rice, J. Chem. Phys. 86, 1036 (1987); A. Bloch and S. A. Rice, Phys. Rev. 185, 933 (1969).

[43]F. Abeles, Ann. Phys. (Paris) 3, 504 (1948); 5, 596 (1950); A. Herpin, C. R. Acad. Sci. 225, 182 (1947).

[44]R. S. Becker, J. A. Golovchenko, and J. R. Patel, Phys. Rev. Lett. 50, 153 (1983).

[45]A. Messiah, Quantum Mechanics, (Wiley, New York, 1962), Vol. 2, pp. 673-675.

[46]S. R. Andrews and R. A. Cowley, J. Phys. C 18, 6247 (1985); I. K. Robinson, Phys. Rev. B 33, 3830 (1986).

[47]K. S. Liang, E. B. Sirota, K. L. D'Amico, G. J. Hughes, and S. K. Sinha, Phys. Rev. Lett. 59, 2447 (1987); J. Villain, D. R. Grempel, and J. Lapujoulade, J. Phys. F 15, 809 (1985); M. den Hijs, E. K. Riedel, E. H. Conrad, and T. Engel, Phys. Rev. Lett. 55, 1698 (1985); 57, 1279 (1986).
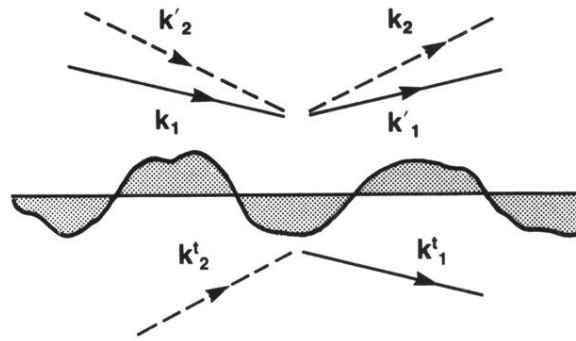
FIG. 4. Schematic of a rough surface. The horizontal line is the average surface ($z=0$). The shaded regions are the regions of perturbation to a smooth surface. The incident wave vectors $\mathbf{k}_1$ and $-\mathbf{k}_2$, the reflected wave vectors $\mathbf{k}_{1'}$ and $-\mathbf{k}_{2'}$, and the transmitted wave vectors $\mathbf{k}_1^t$ and $-\mathbf{k}_2^t$ are illustrated.